Supporting Information

Harvesting the Vibration Energy of $BiFeO_3$ Nanosheets for Hydrogen Evolution

Huilin You, Zheng Wu*, Luohong Zhang, Yiran Ying, Yan Liu, Linfeng Fei, Xinxin Chen, Yanmin Jia*, Yaojin Wang, Feifei Wang, Sheng Ju, Jinli Qiao, Chi-Hang Lam, and Haitao Huang*

DOI: 10.1002/anie.2016XXXXX

Experimental Procedures

Hydrothermal synthesis of $BiFeO_3$ 2.425 g $Bi(NO_3)_3 \cdot 5H_2O$ was dissolved in ethylene glycol solution under vigorous stirring. Once completely dissolved, 1.352 g $FeCl_3 \cdot 6H_2O$ and 200 mL deionized water were added into the solution. The pH value of the solution was adjusted to be 10~11 by dropping $NH_3 \cdot H_2O$ under vigorous stirring. The precipitation was collected by centrifugation, which was then added to 40 mL NaOH solution (5 mol/L) and sealed into a Teflon-lined stainless steel autoclave. The autoclave was heated at 180 ℃ for 48 h, followed by cooling down to room temperature. After that, the products were collected by centrifugation and fully rinsed with deionized water. The final products were obtained by drying at 60 ℃ for 12 h and calcination at 500 °C for 2 h, both in air. All reagents used as starting materials were of analytical grades.

Characterization of catalyst The X-ray diffraction (XRD) patterns of hydrothermally-synthesized $BiFeO_3$ were recorded by Philips PW3040/60 X-ray powder diffractometer (Netherlands) and Rigaku SmartLab (Japan). The morphology of $BiFeO_3$ was studied by a Phenom ProX desktop scanning electron microscopy (SEM, Netherlands) and a JEOL Model JEM-2100F Field Emission Electron Microscope STEM. Atomic force microscopy (AFM, Asylum MFP 3D Infinity) was used to characterize the thickness of the $BiFeO_3$ nanosheet. Energy dispersive X-ray spectroscopy (EDS) mapping was conducted for elemental analysis, using a Phenom EDS detector unit attached to the Phenom ProX desktop SEM. A thin layer of Au was sputtered on the $BiFeO_3$ sample for the better capture of SEM images of the sample and, therefore, Au signal can be detected in the corresponding EDS spectrum. For all the piezo-catalysis experiments that followed, no Au coating was used. Chemical states of the surface elements of $BiFeO_3$ catalyst were determined by an ESCLALAB 250Xi X-ray photoelectron spectroscopy (XPS, USA). Ferroelectric hysteresis loop was measured at room temperature through a ferroelectric analyzer (RTI-Multiferroic-4 kV, Radiant, USA) at 1 kHz. The piezoelectric response of the synthesized $BiFeO_3$ nanosheet was characterized by MFP-3D piezoresponse force microscope (MFP-3D, USA). The Electrochemical tests of $BiFeO_3$ was measured via Solartron Electrochemical Workstation (UK) and Chenhua CHI660e Electrochemical Workstation (China). UV-Vis Diffuse reflectance spectra was tested by SHIMADZU UV-2550 UV-vis spectrophotometer (Japan). The dye decomposition concentrations were determined by measuring the absorption spectra at λ_{max}=484 nm using Hitachi U-3900 UV-vis spectrophotometer (Japan) and a calibration curve.

Hydrogen production experiments The piezo-catalytic hydrogen production of the $BiFeO_3$ nanosheets was evaluated offline. In a typical experiment, 10 mg of the $BiFeO_3$ nanosheets was dispersed in 10 mL of Na_2SO_3 solution (0.05 M). Na_2SO_3 was used as a sacrificial agent. The aqueous suspension sealed in a 25-mL borosilicate tube was evacuated and purged by Ar for about 5 min to completely remove air. Since it is difficult to directly apply a macro stress on a nanosheet, we used ultrasonic vibration to generate an appreciable stress (1.01×10^5 kPa) to bend the $BiFeO_3$ nanosheets via the microbubble explosion force, which has been widely reported. [1] The borosilicate tube was then placed in the center of an ultrasonic bath with different vibration frequency and power. To detect the amount of hydrogen production, 1 mL gas component within the borosilicate tube was intermittently extracted and injected into a gas chromatograph (7890B, USA) with a thermal conductivity detector. The amount of hydrogen gas produced was calculated using a calibration curve of moles of hydrogen versus peak area.

Electrochemical measurement The Electrochemical tests of $BiFeO_3$ was operated in a standard three-electrode configuration with glassy carbon electrode as working electrode, carbon rod as counter electrode, and Hg/Hg_2Cl_2/saturated KCl (SCE) as the reference electrode. In HER performance experiment, 1 M Na_2SO_4 (pH=7) was used as the electrolyte. In Mott-Schottky test, 0.1 M Na_2SO_4 (pH=6.8) was used as the electrolyte. The electrode potential versus saturated calomel electrode (SCE) was converted to reversible hydrogen electrode (RHE) potential according to the Nernst equation: $V_{RHE}=V_{SCE}+0.059\times pH+V^0_{SCE}$, in which $V^0_{SCE}=0.245V$ at pH=6.8, 25°C, and V_{SCE} was the potential obtained against Hg/Hg_2Cl_2/saturated KCl reference electrode.[1]

Results and Discussion

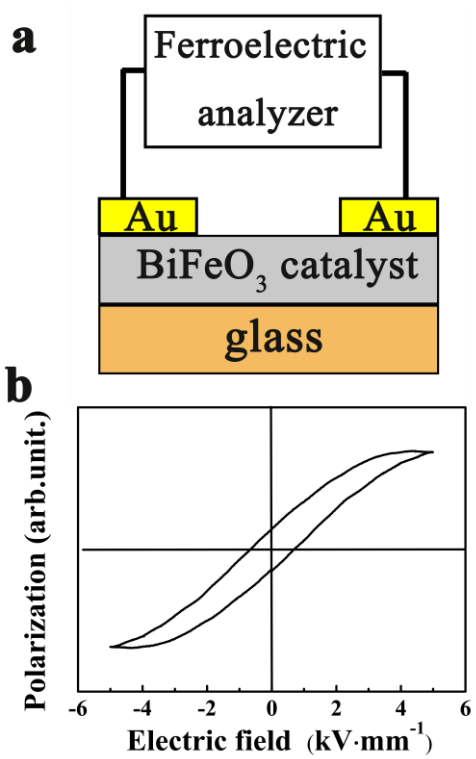

Figure S1 Ferroelectric characterization of $BiFeO_3$. **a** Schematic experimental set-up for the *P-E* hysteresis loop measurement. **b** *P-E* hysteresis loop of $BiFeO_3$.

The polarization versus electric field curve (*P-E* hysteresis loop) of $BiFeO_3$ was traced at a frequency of 1 kHz. Figure S1a is a schematic diagram displaying the circuit of the *P-E* loop measurement, where the $BiFeO_3$ catalyst film was laid on a glass substrate and Au acts as the two electrodes. When the applied electric field increases to 5 $kV \cdot mm^{-1}$, the polarization reaches saturation with an obvious hysteresis loop as shown in Figure S1b, indicating the ferroelectric nature of $BiFeO_3$.

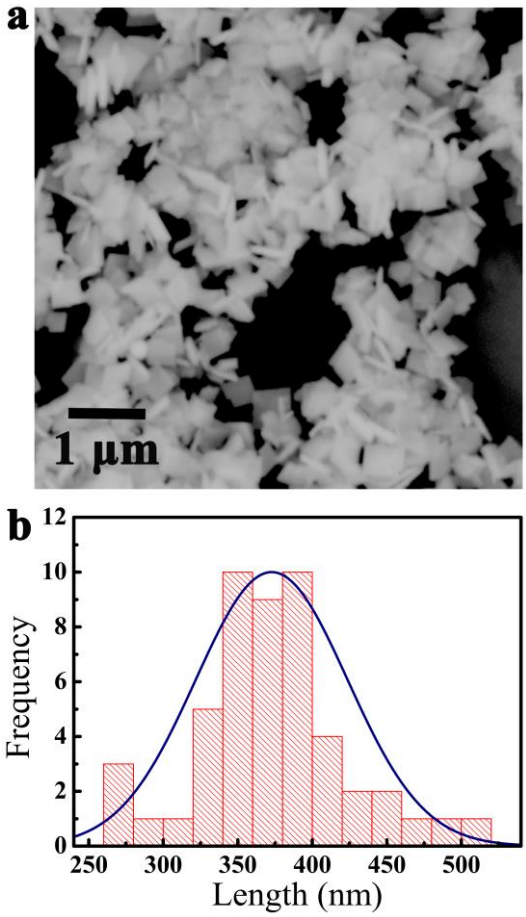

Figure S2. a SEM image and **b** Size distribution of the $BiFeO_3$ nanosheets.

As shown in Figure S2, the average particle size of the $BiFeO_3$ nanosheets was found to be 372.7 ± 50.98 nm.

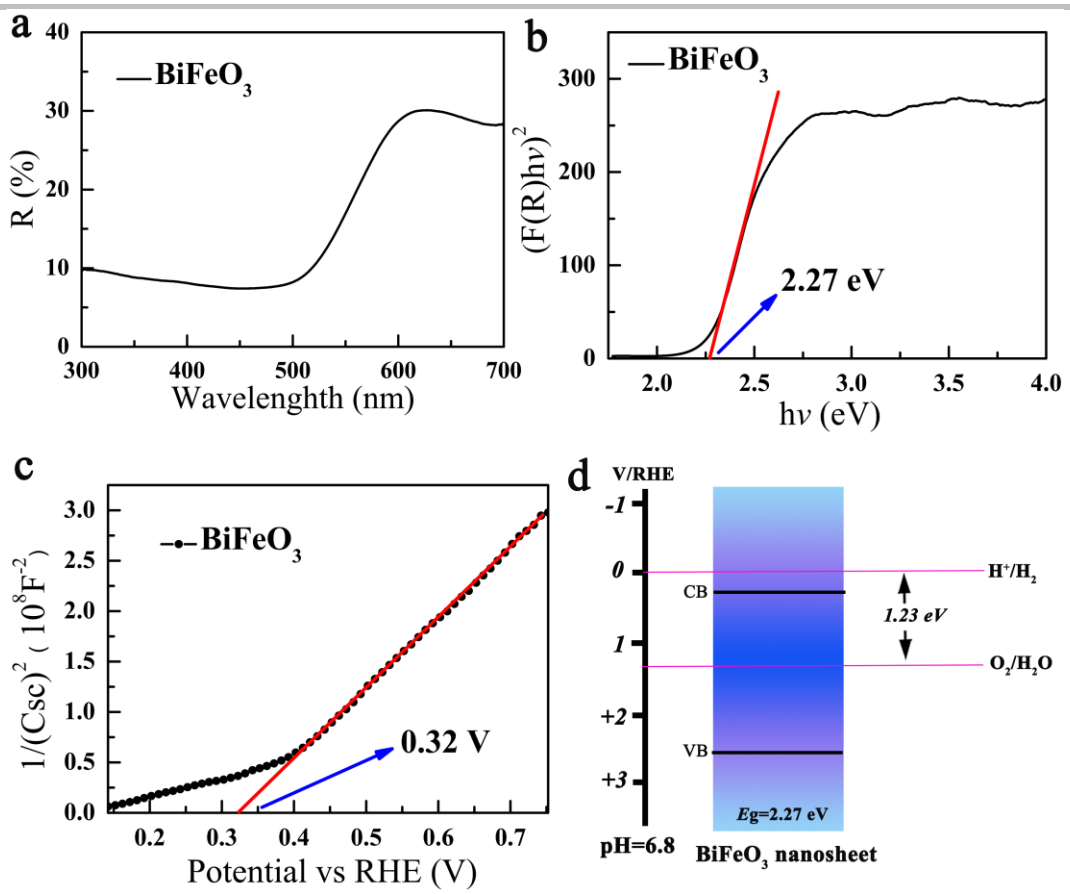

Figure S3. (a) UV-Vis diffuse reflectance spectra, (b) Tauc's plots, (c) Mott-Schottky curves, and (d) Energy band diagram of the as-prepared $BiFeO_3$ nanosheets.

To have a complete understanding of the band alignment, UV-Vis diffuse reflectance spectra and Mott-Schottky spectra were conducted. UV-Vis diffuse reflectance spectra of the as-prepared $BiFeO_3$ nanosheets is shown in Figure S3a. According to Tauc relationship and Kubelka-Munk equation, the energy bandgap (E_g) of material can be estimated by the following equations [2]:

$$F(R)h\nu = A(h\nu - E_g)^n \quad (1)$$

$$F(R) = \frac{(1-R)^2}{2R} \quad (2)$$

where $F(R)$ is the so-called remission or Kubelka-Munk function, R is reflectance, h is the Planck's constant, ν is the photon frequency, A is a constant. E_g is the energy bandgap, and n is selected as 0.5 or 2 for direct and indirect bandgap materials, respectively. In our case, 0.5 is chosen for $BiFeO_3$ with a direct bandgap. As shown in Figure S3b, the energy bandgap of our synthesized $BiFeO_3$ is 2.27 eV, which is responsive to visible light. The flat band potential at the electrode-electrolyte interface can be estimated by the following Mott-Schottky equation [1]:

$$\frac{1}{C^2} = \frac{2}{\varepsilon_r \varepsilon_0 e N_d A^2}\left[(V - V_{fb}) - \frac{kT}{e}\right] \quad (3)$$

where C is the specific capacity, ε_r and ε_0 are the dielectric constants of the catalyst and vacuum, respectively, e is elemental charge and N_d is the number of donors in the catalyst, A is the effective area of electrode, V is the applied potential, and V_{fb} is the flat band potential, k is the Boltzmann constant, and T is the absolute temperature. The as-prepared $BiFeO_3$ nanosheets were loaded onto a glassy carbon electrode with a mass loading of 2 $mg \cdot cm^{-2}$. As shown in Figure S3c, a flat band potential of 0.32 V *vs*. RHE can be estimated from the *x*-intercept of the linear region of Mott-Schottky plot. The Mott-Schottky spectra of $BiFeO_3$ under constant frequency of 1 kHz shows a positive slope of the line segment, revealing *n*-type characteristics for our synthesized $BiFeO_3$. Since for *n*-type semiconductor the conduction band (CB) is generally 0.1-0.3 V more negative than the flat band potential, the CB of $BiFeO_3$ is regarded to be slightly below the redox potential for hydrogen evolution[3]. The schematic energy band diagram of the synthesized $BiFeO_3$ nanosheet is shown in Figure S3d.

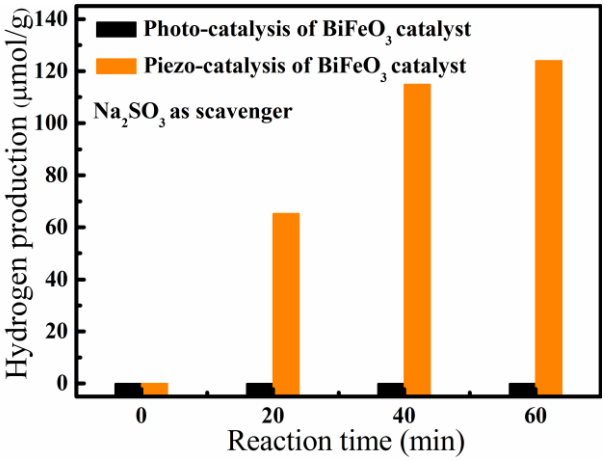

Figure S4. The hydrogen production from water splitting by $BiFeO_3$ nanosheets with different stimulated sources.

We further verify that there is no photo-catalytic hydrogen production activity of our $BiFeO_3$ nanosheets due to the slightly more positive conduction band edge than the redox potential for hydrogen evolution (H_2/H_2O). We dispersed 100 mg $BiFeO_3$ nanosheets in 100 mL of Na_2SO_3 solution (0.05 M). The solution was then put into a reactor. The incident light was from a 300 W Xe lamp, which was filtered to match the AM 1.5G spectrum. The distance between reactor and lamp is around 3 cm. Before photo-catalysis, the reactor was evacuated to completely remove the air. As shown in Figure S4, with increasing photo-catalytic time, there is no hydrogen production, in comparison with the piezo-catalytic hydrogen evolution.

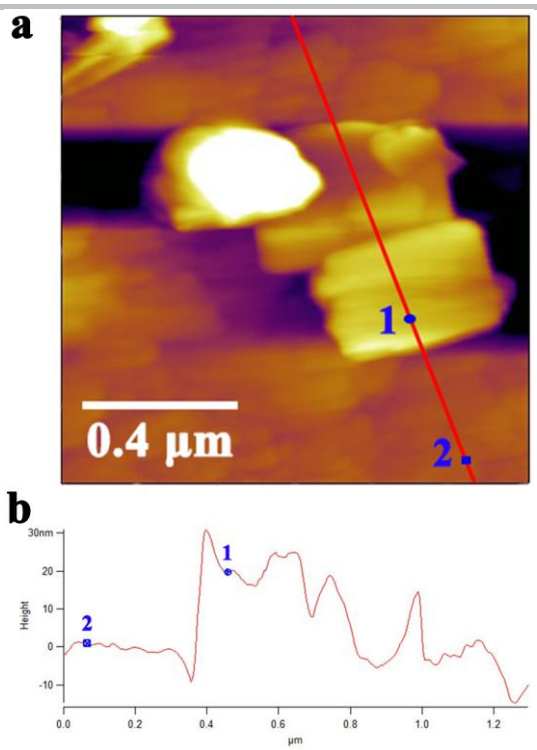

Figure S5 a AFM image of the $BiFeO_3$ nanosheets. **b** Line profile along the red line in the AFM image, which reveals a thickness of ~20 nm.

Atomic force microscopy (AFM) was used to characterize the thickness of the $BiFeO_3$ nanosheet. The $BiFeO_3$ nanosheet was clearly observed in the AFM image (Figure S5a). Figure S5b is the line profile along the red line in the AFM image, which indicates that the thickness of the $BiFeO_3$ nanosheet is around 20 nm.

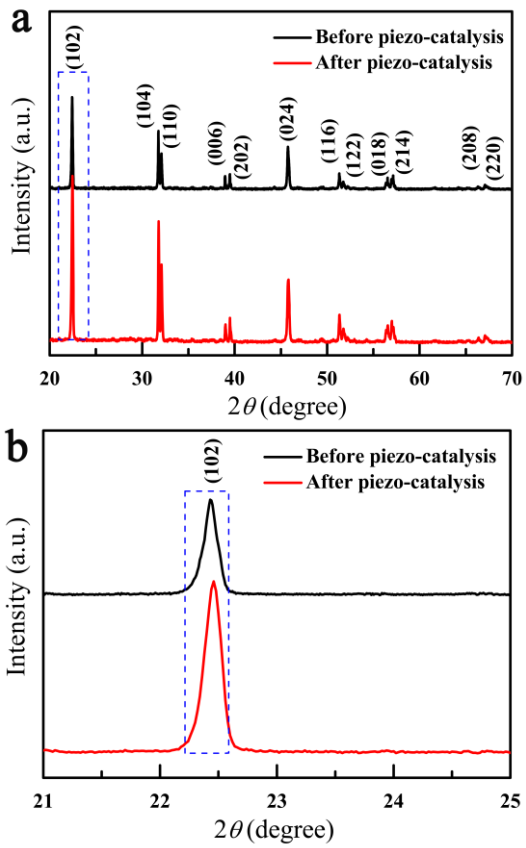

Figure S6. (a) XRD patterns and (b) expanded (102) diffraction peaks of $BiFeO_3$ nanosheets before and after the piezo-catalysis.

As shown in Figure S6, XRD patterns of $BiFeO_3$ nanosheets before and after the 60 min piezo-catalysis are quite similar and no secondary phases can be detected. The particle size (D) can be roughly estimated with the well-known Debye-Scherrer Formula[4]:

$$D = \frac{K\lambda}{\beta \cos\theta} \tag{4}$$

where K equals 0.89 and λ is the wavelength. β is the full width at half maximum (FWHM) intensity and θ is the Bragg diffraction angle. According to the FWHM of the (102) peak of $BiFeO_3$, the particle size is roughly estimated to be 218.15 nm before piezo-catalysis and 157.58 nm after piezo-catalysis, which agrees well with the TEM results before and after piezo-catalysis (Figure 2 of the manuscript and Figure S7 of the supporting information).

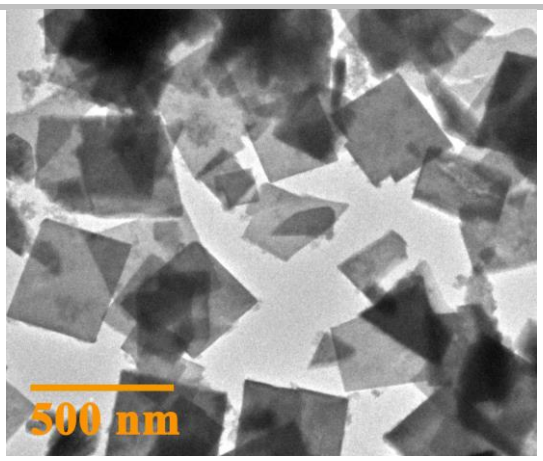

Figure S7. TEM bright-field image of $BiFeO_3$ nanosheets after the piezo-catalysis.

Figure S7 shows that after piezo-catalysis for 60 mins, a number of cracked nanosheets were generated due to the high power (100 W) of the ultrasonic machine used. Working at the resonant frequency is another reason that the $BiFeO_3$ nanosheets are easily cracked. This result agrees well with the experimental result (Figure 5) that the hydrogen production rate decreases with increasing reaction time. Decreasing the ultrasound power and tuning the frequency away from resonance will reduce the number of cracked nanosheets.

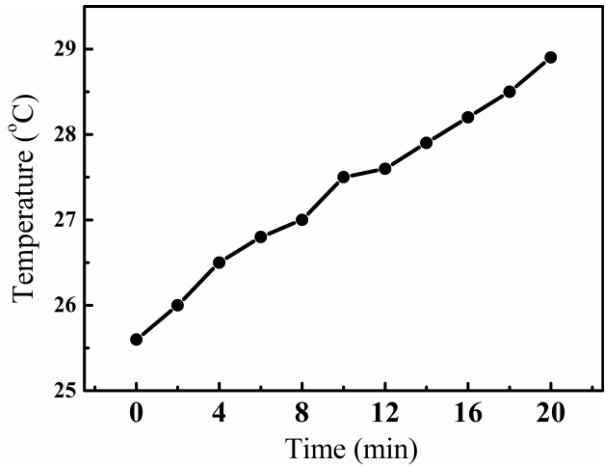

Figure S8 Temperature variation of water during ultrasonication.

As shown in Figure S8, the water temperature change rate was 0.33 °C·min^{-1}. The water in the ultrasonic bath was changed every 20 min. The temperature variation is kept to be below 4 °C.

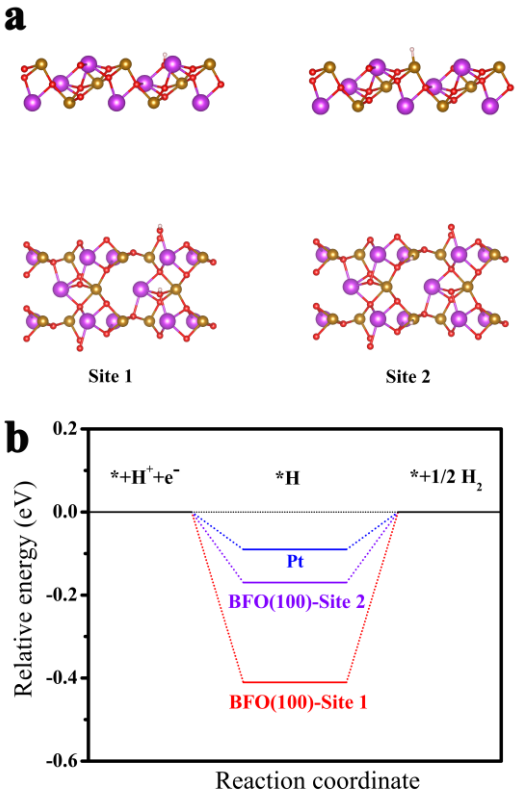

Figure S9 a Optimized crystal structures with one H atom adsorbed onto Site 1 and Site 2 on the (100) surface of BFO. The purple spheres (largest size), yellow spheres (middle size) and red spheres (smallest) represent Bi, Fe and O, respectively. **b** Diagram of adsorption energy for H on the (100) surface of BFO with comparison to that on Pt.

According to the electron diffraction pattern (inset of Figure 2b), the most exposed facet of our $BiFeO_3$ (BFO) is found to be the (100) plane. Density functional theory (DFT) calculations was then carried out to study the protonation of the (100) surface of BFO nanosheets. Two adsorption sites were identified on the (100) surface of BFO (denoted as Site 1 and Site 2 (Figure S9a)). The adsorption energy values of H atom on the two sites are -0.41 and -0.17 eV, respectively, indicating that the H adsorption is energetically favorable on the (100) surface of BFO (Figure S9b).

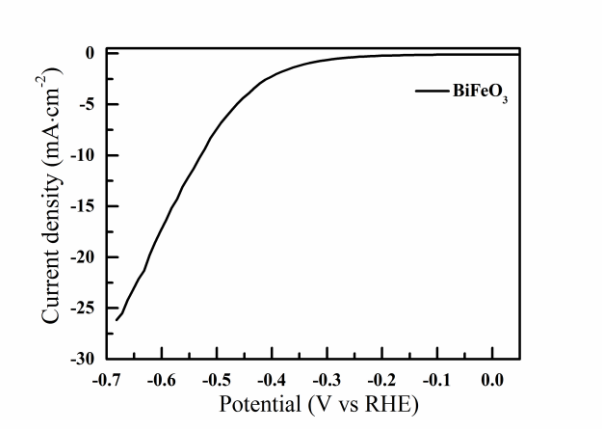

Figure S10 Polarization curves for HER on modified glassy carbon electrodes comprising $BiFeO_3$ nanosheets in 1 M Na_2SO_4 solution.

Furthermore, to provide direct evidence of the electro-catalytic activity of $BiFeO_3$ towards hydrogen production, we measured the HER performance of $BiFeO_3$ nanosheets. The as-prepared $BiFeO_3$ nanosheets were loaded onto a glassy carbon electrode with a mass loading of 1.41 $mg \cdot cm^{-2}$. Figure S10 displays $BiFeO_3$ nanosheets' polarization curves in 1 M Na_2SO_4 solution. Hydrogen evolution can be clearly observed at a potential above ~400 mV.

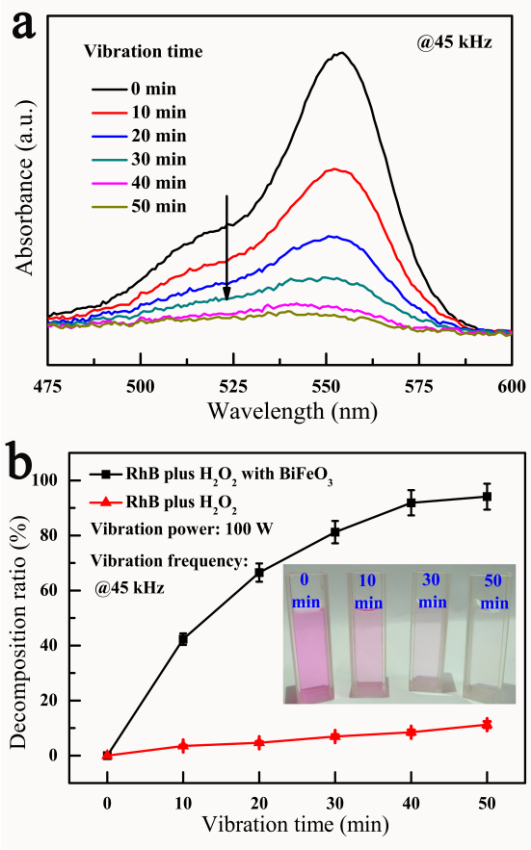

Figure S11 The piezo-catalytic dye decomposition experiment. **a** The absorption spectra of RhB dye solution (5 mg/L) with the addition of $BiFeO_3$ square nanosheets after experiencing different vibration time. **b** Piezo-catalytic RhB dye decomposition ratio as a function of vibration time. The

inset shows the photos of the piezo-catalytically decomposed RhB dye solution after different vibration time.

The piezo-catalytic dye decomposition experiments were carried out in Rhodamine B (RhB) dye solutions (5 mg·L^{-1}). It is not easy to impose a macro stress directly onto nano-particles. Hence, an ultrasonic source with a frequency of ~45 kHz was employed to generate mechanical stress onto the $BiFeO_3$ nanosheets. The method of exerting stress on micro-/nanoparticles via ultrasonic cavitation has been widely reported[5]. 50 mg $BiFeO_3$ nanosheets and 50 mL RhB dye solution were contained in a glass beaker set at the center of an ultrasonic bath with a dark environment to avoid possible photocatalytic decomposition. 0.5 ml H_2O_2 was added to increase reaction rate. The dye solution samples were collected by centrifugation after each specific vibration time interval. No sacrificial agent was used in the piezo-catalytic dye decomposotion experiment.

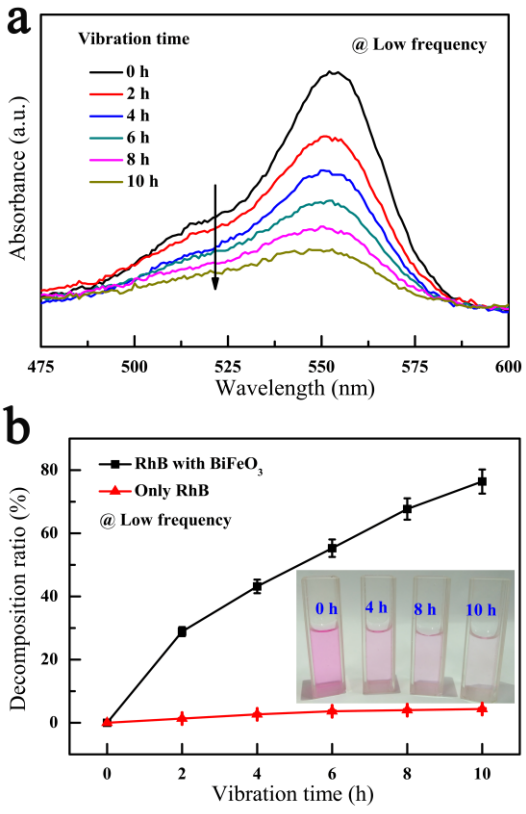

Figure S12 The low frequency piezo-catalytic dye decomposition experiments **a** The absorption spectra of RhB dye solution (5 mg/L) with the addition of $BiFeO_3$ square nanosheets after experiencing different low frequency vibration time. **b** The low frequency piezo-catalytic RhB dye decomposition ratio as a function of vibration time. The inset shows the photos of the low frequency piezo-catalytically decomposed RhB dye solution after different vibration time.

The low frequency piezo-catalytic decomposition of RhB dye was conducted by slow stirring of the solution containing $BiFeO_3$ nanosheets. First, 150 mg $BiFeO_3$ nanosheets were added into 50 mL (5 $mg \cdot L^{-1}$) RhB solution. The suspension was then stirred by magnetic stirrer at a rotational speed of 600 rpm in dark to eliminate possible photocatalytic reaction. Because the stirring is gentle, no additional temperature control is needed to keep the solution temperature constant (at room temperature). 3 mL of suspension was taken out from the mixed solution after each 2 h magnetic stirring. The dye decomposition concentrations were determined in a way similar to the above. No sacrificial agent or H_2O_2 was used in the piezo-catalytic dye decomposotion experiment.

Energy Balance Model:

For an energy conversion system, it is always important to evaluate the conversion efficiency of the system. The efficiency of piezo-catalytic hydrogen evolution can be evaluated by the following energy balance model,

$$Q_{input} - Q_{loss} = Q_{store} \quad (5)$$

where Q_{input} denotes the actual mechanical energy captured by the piezo-catalyst through the mechanical vibration; Q_{loss} accounts for the energy losses due to generation of heat, recombination of the piezo-induced electrical charges, and surplus energy used in the formation of hydrogen (such as overpotential), etc.; and Q_{store} denotes the stored energy in the form of hydrogen gas. While it is relatively easy to quantify Q_{store} by measuring the amount of hydrogen evolution, it is not an easy task to determine the actual mechanical energy captured by the piezo-catalyst. Q_{input} cannot be simply calculated by the power of the ultrasonic source we used. One has to consider the mechanical energy loss during transmission and the loss due to different acoustic impedances at the interfaces of two different materials. One also has to consider the small cross-section and volume of the piezo-catalyst as compared with the surrounding liquid, where a large amount of mechanical energy is actually not utilized. We would like to leave the quantitative calculation of Q_{input} as an open question.

The value of the output chemical energy of a single $BiFeO_3$ nanosheet can be simply calculated as,

$$E_{chem} = \frac{2nV_t N_A e}{N}$$

where n= hydrogen produced in moles; V_t = threshold voltage (1.23 V) for water splitting; N_A = Avogadro's number; e = elemental charge; N= number of nanosheets.

The number of nanosheets can be estimated as,

$$N = \frac{m}{\rho \cdot V} = \frac{1g}{8344kg \cdot m^{-3} \times 380nm \times 380nm \times 20nm} = 4.15 \times 10^{13}$$

where ρ=density of $BiFeO_3$ (8344 kg/m^3). The width and thickness of nanosheet are 380 and 20 nm, respectively. According to the above equations, the chemical energy output of a single $BiFeO_3$ nanosheet per second in the present case is:

$$E_{chem} = \frac{2nV_t N_A e}{N} = \frac{2\times 3.45\times 10^{-8}\times 1.23\times 6.02\times 10^{23}\times 1.602\times 10^{-19}(J\cdot s^{-1})}{4.15\times 10^{13}(nanosheet)}$$

$$= 1.97\times 10^{-16} J\cdot s^{-1} nanosheet^{-1}$$

References

[1] J. Ke, J. Liu, H. Sun, H. Zhang, X. Duan, P. Liang, X. Li, M.O. Tadea, S. Liu, S. Wang, *Applied Catalysis B: Environmental*, 2017,200, 47-55.

[2] a) P. Yilmaz, D. Yeo, H. Chang, L. Loh, S. Dunn, *Nanotechnology*, 2016, 27, 345402; b) R.L.Go´mez, *J Sol-Gel Sci Technol*, 2012, 61, 1-7.

[3] W. Chun, A. Ishikawa, H. Fujisawa, T. Takata, J.N. Kondo, M. Hara, M. Kawai, Y. Matsumoto, K. Domen, *J. Phys. Chem. B*, 2003, 107, 1798-1803.

[4] P. Scherrer, Bestimmung der inneren Struktur und der Größe von Kolloidteilchen mittels Röntgenstrahlen. In: Kolloidchemie Ein Lehrbuch. Chemische Technologie in Einzeldarstellungen. Springer, Berlin, Heidelberg (1912).

[5] a) N.C. Eddingsaas, K.S. Suslick, *Nature*, **2006**, *444*, 163-163; b) C.R. Hickenboth, J.S. Moore, S.R. White, N.R. Sottos, J. Baudry, S.R. Wilson, *Nature*, **2007**, *446*, 423-427; c) X.D. Wang, J.H. Song, J. Liu, Z.L. Wang, *Science*, **2007**, *316*, 102-105.